Meteorology and Atmospheric Physics (2024) 136:15
https://doi.org/10.1007/s00703-024-01011-5

ORIGINAL PAPER

Aerosol optical depth and water vapor variability assessed through autocorrelation analysis

Marco A. Franco[1,3] · Fernando G. Morais[1] · Luciana V. Rizzo[1] · Rafael Palácios[2] · Rafael Valiati[1] · Márcio Teixeira[1] · Luiz A. T. Machado[1] · Paulo Artaxo[1]

Received: 6 June 2023 / Accepted: 20 February 2024 / Published online: 31 March 2024

Abstract

Numerous studies globally have centered on atmospheric air pollution due to its profound health and climate effects. NASA's AERONET (National Aeronautics and Space Administration - AErosol RObotic NETwork) network has been one of the world's leading tools for accessing the physical properties of atmospheric aerosols from various sources, mainly anthropogenic ones. This study proposes a new approach to evaluate the Aerosol Optical Depth (AOD) and precipitable water vapor (PWV) seasonality and the influence of short-term perturbations, such as the presence of local and regional aerosol sources or meteorological events, based on the temporal autocorrelation function (ACF). We introduce the adimensional seasonal assessment autocorrelation function, $\Delta_{ACF,k}$, as a parameter to quantify the influence of the short-term perturbation, and we use its average, $\langle\Delta_{ACF,k}\rangle$, as a proxy for seasonality loss. The smaller $\langle\Delta_{ACF,k}\rangle$, the lower the influence of high-frequency perturbations on seasonality. Nine AERONET network sites in South America with different environmental characteristics were evaluated. The selected sites were São Paulo, Rio Branco, Manaus, ATTO (Amazon Tall Tower Observatory), AltaFloresta, Ji-Paraná, Cuiabá, Buenos Aires, and La Paz. The results showed that sites with less local anthropogenic aerosol sources acting as short-term perturbations had pronounced AOD seasonality and a linear relationship between the ACF functions of AOD, PWV, and the simulated direct solar radiation. As local anthropogenic sources become more prominent, the AOD ACF is attenuated and has less amplitude in seasonal oscillations. In addition, the relationship between AOD and PWV ACF becomes more attenuated. Buenos Aires has shown to be the most affected site, with $\langle\Delta_{ACF,AOD}\rangle$ of 0.47, followed by São Paulo and La Paz. The areas in the Amazonian deforestation arc had relatively close average $\Delta_{ACF,AOD}$, with Alta Floresta representing the most influenced by short-term perturbations. Central Amazonian sites had the lowest $\Delta_{ACF,AOD}$ averages, of about 0.25, which means that constant local anthropogenic sources do not dominate the AOD seasonality and that the wet deposition still plays an essential role in regulating the aerosol sources in the atmosphere. In contrast, the behavior of $\langle\Delta_{ACF,PWV}\rangle$ in the Amazon region varies mainly due to meteorological influences, with the highest values observed in the central region, likely related to the high amount of water vapor in the atmosphere, and more pronounced seasonality near deforestation arcs and major cities. The proposed method eliminates the need for a reference site when comparing seasonalities of different time series, enabling valid comparisons across different areas without a comparative reference point. The method can be further applied to other atmospheric time series, including greenhouse gases.

Responsible Editor: Clemens Simmer Ph.D.

✉ Marco A. Franco
marco.franco@usp.br

[1] Institute of Physics, University of São Paulo, São Paulo, SP, Brazil

[2] Faculdade de Meteorologia, Instituto de Geociências, Universidade Federal do Pará, Belém 66075-110, Brazil

[3] Present Address: Department of Atmospheric Sciences, Institute of Astronomy, Geophysics and Atmospheric Sciences, University of São Paulo, Rua do Matão, 1226, Cidade Universitária, São Paulo 05508-090, Brazil

1 Introduction

Atmospheric air pollution has been the focus of several studies in different regions since its impacts on the environment, climate, and health are highly significant (Bernstein et al. 2004; Carracedo-Martínez et al. 2010). Air pollution has serious health effects on humans and animals (Kampa and Castanas 2008). Exposure to high levels of pollutants such as particulate matter (PM), ozone (O_3), and nitrogen oxides (NO_x) can lead to respiratory and cardiovascular diseases, as well as cancer (Manisalidis et al. 2020; Næss et al. 2007;

Ribeiro et al. 2019). By studying air pollution, scientists and policymakers can better understand the health risks associated with exposure and take steps to reduce exposure and protect public health.

Atmospheric aerosols can be emitted directly from the source (primary aerosols) or be formed in the atmosphere (secondary aerosols) (Seinfeld and Pandis 2016). Regardless of the emissions and formation mechanism, they can remain in the atmosphere for periods from a few hours to a few weeks. Air masses can even transport them from one continent to another, crossing large ocean regions (Holanda et al. 2020, 2023). The atmosphere is a complex system driven mainly by solar radiation, which modulates processes at different spatial and temporal scales (Seinfeld and Pandis 2016). Seasonal variations are associated with climate and regional emissions, while variations with shorter periods usually indicate short-term perturbations. Pollutant concentrations at a specific atmospheric region arise from overlapping processes across various temporal and spatial scales.

Urban regions are an intense and constant source of atmospheric aerosols, either by secondary formation due to the presence of reactive compounds such as O_3 and NO_x radicals or by direct emission from vehicle exhausts (Brito et al. 2018). In megacities like São Paulo, Brazil, with a population of ~ 20 million inhabitants in its metropolitan area, the concentration of atmospheric aerosols is, on average, of ~ 12,000 cm^{-3} (dos Santos et al. 2016; Monteiro dos Santos et al. 2021). Many studies have shown that vehicular emissions in São Paulo considerably contribute to air pollution (Monteiro dos Santos et al. 2021; Brito et al. 2018). In highly polluted cities, such as many of them in China and India, the high atmospheric aerosol concentration causes breathing problems and radically affects vision (Cheung et al. 2005; Tiwari et al. 2011).

In contrast, in tropical forests like the Amazon, the predominant sources of aerosols depend directly on the availability of rain. In the wet season, isolated places such as the Amazon Tall Tower Observatory (ATTO) (Andreae et al. 2015) in central Amazon present very low aerosol concentrations of ~ 300 cm^{-3}, and the aerosol number concentration in the atmosphere is mainly dominated by secondary organic aerosols formed locally and regionally (Andreae et al. 2018; Franco et al. 2022). Urban sites close to or in the forest, such as Manaus, have their atmosphere influenced by urban emissions, which even favor the formation of secondary aerosols far away from the forest (Nascimento et al. 2021, 2022). However, significant aerosol plumes affect urban and isolated Amazonian sites due to local and regional biomass burning during the dry season. This influence depends more on the distance of these sites from the sources, in which particle concentrations can easily exceed 10,000 cm^{-3} (Artaxo et al. 2002; Franco et al. 2022; Ponczek et al. 2022). The aerosol load is so intense that it can make Amazonian sites equally or even more polluted in specific periods than most densely populated cities.

NASA's AERONET (National Aeronautics and Space Administration - AErosol RObotic NETwork) project has been one of the world's leading tools to provide direct access to concentrations and physical properties of aerosols and precipitable water vapor content in the atmosphere. The network has photometers installed in several places around the planet, whether they are remote regions such as the Amazon, Antarctica, and the Sahara desert or even rural, urban, coastal, and island areas (da Silva Palácios et al. 2020; Kambezidis and Kaskaoutis 2008; Kaskaoutis et al. 2007; Holben et al. 1998). This makes AERONET one of the main tools for scientists to study atmospheric aerosols' seasonal behaviors and their impacts under different environmental conditions. The aerosol optical depth (AOD) seasonality is fundamental in understanding the effects of the various sources that contribute to the atmospheric particulate load (Morais et al. 2022). AERONET is frequently utilized to validate data obtained from satellites. It assists in proposing corrections aimed at enhancing the accuracy of satellite data (Palácios et al. 2022; Carra et al. 2020; Zhao et al. 2002; Prasad and Singh 2009). Therefore, high-frequency variations in the AOD signal, also seen as short-term perturbations, broadly indicate local and regional disturbances or emissions. Human activities, such as burning fossil fuels and emitting industrial pollutants, or natural events, such as forest fires or volcanic eruptions, can cause these disturbances. It is essential to understand how these different processes affect air quality at different scales to develop effective strategies for monitoring and mitigating pollutants.

Studying AOD seasonality with statistics is fundamental because AOD is an indirect measure of the aerosol load in the atmosphere (da Silva Palácios et al. 2020; Artaxo et al. 2022). Using statistical methods to analyze AOD data makes it possible to understand and evaluate the patterns of aerosol concentrations over time, including any seasonal variations. This information can be used to improve air quality forecasts and predictions and develop better regulations related to air pollution. Furthermore, AOD is also important for assessing the radiative forcing of the Earth's atmosphere, which measures the difference in energy absorbed by the Earth's system and energy reflected in outer space (Seinfeld and Pandis 2016). Understanding the seasonality of AOD can help better understand the Earth's energy balance, which is crucial for climate change research.

Traditionally, the study of seasonality involves decomposing a time series into its periodic behavior and trend components. By measuring the amplitude of the periodic oscillation by calculating the maximum and minimum values, an indication of the degree of seasonality can be obtained (Nworof and Chineka 2007). However, this

method only provides relative comparisons between sites, making it difficult to obtain absolute comparisons between, for example, different studies. This lack of standardization generates challenges when attempting to synthesize results from multiple studies or comparing results across other regions or periods. To overcome these challenges, there is a need for a standardized and universally applicable method for quantifying seasonality that can provide absolute comparisons between sites.

A few studies use autocorrelation to assess the seasonal behavior of AOD and column-integrated water vapor in the atmosphere (PWV). However, most of them use the technique to access the performance of a regional model for predicting PM2.5 (Chau et al. 2021) or to investigate spatial and temporal relationships between AODs of different locations (Hua et al. 2016; Yang and Hu 2018). None investigated the temporal autocorrelation seasonal variability of AOD and PWV, particularly in South America. Studying environmental sites in South America with different aerosol sources and meteorological conditions is crucial for understanding the impact of aerosols on air quality, visibility, climate, and human health in the region. It enables researchers to characterize aerosols' composition and infer the contribution of different sources, such as industrial emissions and natural, to the environment.

This study proposes a new approach to evaluate the AOD and PWV seasonalities based on the seasonal pattern of the simulated direct local solar radiation. This is performed from a statistical perspective with the temporal autocorrelation function. We use time series with daily averages of AOD and PWV obtained through the AERONET network in nine sites in South America, with at least seven years of continuous measurements. The sites were categorized into three subgroups: two sites representing tropical Amazonian forested conditions, four sites representing a mixture of urban and forested Amazonian conditions, where biomass-burning aerosol plumes play an important role mainly during the dry season, and three sites representing strong urban conditions. We simulate the direct solar radiation time series for each site through radiative transfer calculations. This data serves as a seasonal time series reference, devoid of meteorological and other atmospheric influences. It provides a consistent representation of direct solar radiation specific to each location.

2 Methodology

This section describes the AERONET photometers used to obtain the AOD and PWV measurements, the environmental conditions of the AERONET sites considered in this study, and the approach applied to calculate the statistical correlations based on the autocorrelation function.

2.1 AERONET sun and lunar photometers

The AERONET network is a NASA measurement program that uses remote sensing to monitor optical and physical parameters of atmospheric aerosols and precipitable water vapor content. In particular, AOD, absorption AOD (AAOD), and precipitable water vapor in the atmosphere are applied to air quality monitoring (Chu et al. 2016; Jin et al. 2019). AERONET uses automatic solar and lunar spectral radiometers, model CIMEL Electronic 318, which allow continuous measurements every 5 min. From the incident solar radiation, the AERONET's algorithm can obtain the extinction coefficient ($\sigma_{\text{ext},\lambda}$) and, therefore, the AOD, which is the integral of $\sigma_{\text{ext},\lambda}$ over the atmospheric vertical profile, as defined below

$$\text{AOD} = \int_{\text{surface}}^{\text{top of atmosphere}} \sigma_{\text{ext}}(z)\, dz. \tag{1}$$

The AERONET algorithm can automatically model the absorption and scattering of radiation through approximations in the geometry of the aerosol particles. They are generally divided into two subcategories: spherical and non-spherical aerosols. The Mie scattering theory is considered for the spherical ones, in which the particles are homogeneous spheres (e.g., with the same complex refractive index for all particles, regardless of size) of different diameters. In the case of non-spherical particles, a method based on the Scattering Matrix Modeling is applied, assuming that these aerosol particles have spheroidal shapes, are homogeneous, and are randomly oriented (Dubovik et al. 2006). The algorithm also considers whether the measurements are direct or indirect (inversions). Direct measurements are obtained from the radiance, made with the collimator of the radiometer pointed at the solar disk, and provide data on the aerosol optical depth and the scattering Ångström exponent.

Indirect measurements, obtained by inversion algorithms with a photometer from diffuse radiance data, allow knowing the size distribution of the aerosols, the effective radius of the distribution, the complex refractive index of the particle (obtained with the scattering and absorption components), and the water vapor content in the atmosphere. AERONET uses the near-infrared (NIR) wavelength region (typically around 940 nm) to measure atmospheric water vapor content. This wavelength region is chosen because it is minimally affected by other atmospheric constituents and provides a strong signal for water vapor absorption. By measuring the intensity of sunlight in this wavelength region and using algorithms to correct for other atmospheric effects,

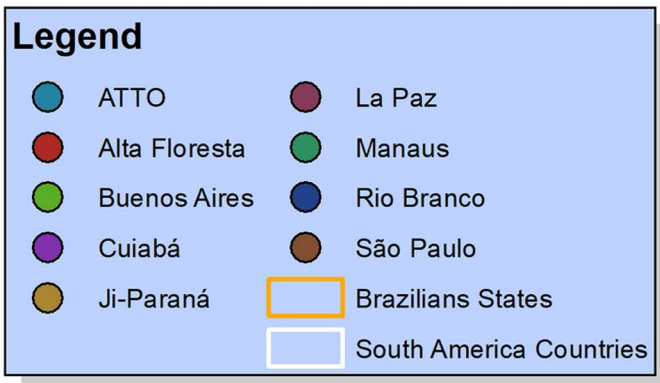

Site	Coordinate		Coverd period
	Coord Y	Coord X	
Alta Floresta	-9,908	-56,064	1999-2021
ATTO	-2,144	-59,000	2016-2022
Buenos Aires	-34,555	-58,506	1999-2022
Cuiabá	-15,731	-56,071	2001-2022
Ji-Paraná	-10,934	-61,852	2006-2020
La Paz	-16,539	-68,066	2006-2022
Manaus	-2,891	-59,97	2011-2019
Rio Branco	-9,957	-67,869	2000-2022
São Paulo	-23,561	-46,735	2000-2022

◂**Fig. 1** AERONET sites throughout South America selected for this study. Their coordinates and AERONET data coverage information are presented in the table on the left side

AERONET can accurately estimate the amount of water vapor present in the atmosphere. It is worth mentioning that the instruments of the AERONET network returned to NASA approximately every year for calibration and testing. All data collected by the various photometers around the planet can be freely downloaded online (https://aeronet.gsfc.nasa.gov/).

2.2 AERONET sites

This study evaluated nine AERONET sites across South America, whose geographical distributions are shown in Fig. 1. The sites were chosen where the AOD and PWV time series were long and robust enough for statistical significance and whose sources of aerosols were more diversified between natural, urban, and biomass-burning emissions. We defined at least seven years of continuous AERONET measurements as the minimum period to fulfill the specified criteria. All AOD and PWV data were obtained at level 1.5 because many sites did not have data processed at level 2.0. This becomes particularly significant when considering that level 2.0 typically underestimates seasonal PWV because of the absence of measurements during cloudy conditions, which represent the wettest and highest PWV periods. In addition, the data were obtained at the daily average level. Figure 1 also presents the sites, their geographic coordinates, and the coverage period of measurements obtained by the AERONET network photometers.

Alta Floresta, ATTO, Cuiabá, Ji-Paraná, Manaus, and Rio Branco are sites located close to or in the Amazon rainforest but with different patterns of aerosol source emissions. ATTO and Manaus, located in the central Amazon, represent the cleanest tropical rainforest. It is worth mentioning that the Manaus AERONET site was located about 30 km northeast of the city and represented quite well-forested conditions. Alta Floresta, Cuiabá, Ji-Paraná, and Rio Branco represent sites inside the deforestation arc, with strong local and regional biomass burning events, especially during the dry season. More details of these six Amazonian sites can be found elsewhere (Morais et al. 2022; Palácios et al. 2022; da Silva Palácios et al. 2020; Artaxo et al. 2022).

São Paulo is a megacity located in southeastern Brazil, with over 20 million people in its metropolitan area (dos Santos et al. 2016). It falls under the Köppen climate classification as a Cwa type (Alvares et al. 2013). This means it has a humid subtropical climate with hot summers (C) and a dry winter season (w). There's a noticeable distinction between the seasons, with a rainy season typically occurring in the warmer months. São Paulo has faced significant air pollution problems in recent years, mainly due to its high levels of vehicle traffic and industrial activity (Brito et al. 2018; Abe and Miraglia 2016). The most common pollutants in the city include PM, NO_x, O_3, and carbon monoxide (CO) (Brito et al. 2018; Monteiro dos Santos et al. 2021). The Brazilian government has implemented measures to address air pollution in São Paulo, such as regulations for vehicle emissions, promoting alternative transportation options, and improving air quality monitoring and reporting (de Fatima Andrade et al. 2017). However, the city continues to face challenges in improving air quality, and more action may be needed to address ongoing air pollution problems.

La Paz is the administrative capital of Bolivia and is located in the Andes Mountains at an elevation of approximately 3600 ms above sea level. The city has a high-altitude, subtropical plateau climate with relatively cold temperatures and high solar radiation levels. La Paz faces air pollution problems due to its high altitude and mountains around it, which can trap pollutants in the city's atmosphere (Wiedensohler et al. 2018). The city also experiences high vehicle traffic, industrial activity, and residential heating and cooking, contributing to air pollution (Borsdorf and Haller 2020). The most common pollutants in La Paz are PM, NO_x, and sulfur dioxide (SO_2) (Mardoñez et al. 2022; Wiedensohler et al. 2018). In recent years, the Bolivian government has addressed air pollution in La Paz such as implementing regulations for vehicle emissions and promoting alternative transportation options. Still, the city continues to face air quality challenges.

One of the biggest cities in South America is Buenos Aires. The metropolitan region, which consists of 24 districts, covers 3880 km^2 and houses at least about ~13 million people (INDEC 2010). It is situated along the western edge of the de La Plata Estuary. According to the National Weather Service, the area has a moist temperate climate with a mean annual temperature of 18 °C, rainfall from 1000 to 1200 mm, and predominant winds from the east and north. The interaction of meso-synoptic systems and intraseasonal events determines weather conditions over the short and medium term. As São Paulo, on a seasonal level, the weather is influenced by the movement of the semi-permanent South Atlantic subtropical anticyclone, which is modulated by larger-scale phenomena related to climate variability (Cuneo et al. 2022; Oliveira et al. 2022).

2.3 Pysolar: a python library for solar radiation simulation

Pysolar is a robust Python library designed for precise solar geometry calculations (Reda and Andreas 2004; Stafford 2015). It is a valuable tool for obtaining accurate direct solar radiation values for a specific location. The library

also provides functions to determine the sun's position and incidence angles relative to a particular point on the Earth's surface. The library allows the obtaining of direct, diffuse, and total solar radiation and solar energy incident on tilted surfaces. Direct solar radiation represents the amount of solar energy that arrives at the Earth's surface directly from the sun, given in W/m^2. The time series of solar radiation derived from Pysolar is free from local and regional influences and considers a clear sky condition.

2.4 Statistical autocorrelation data analysis

Autocorrelation is a statistical procedure that describes the correlation of a time series with itself at different time lags (Hair 2011). It is often used to determine the presence of temporal dependencies in a time series, such as a gradual decay or periodicity. The autocorrelation function (ACF) measures the similarity between a time series and a lagged version of itself. The autocorrelation coefficient at lag k, denoted as ρ_k, measures the correlation between the time series and its lagged version at lag k. The following equation gives the mathematical representation of the ACF

$$\mathrm{ACF}(k) = \rho_k = \frac{\gamma_k}{\gamma_0}, \tag{2}$$

where k is the lag, γ_k is the k-th order autocovariance, and γ_0 is the 0-th order autocovariance, which is simple the variace.

The following expression gives the autocovariance

$$\gamma_k = E[(X_t - \mu)(X_{t-k} - \mu)], \tag{3}$$

where Xt is the time series at time t, μ is the mean of the time series, and E is the expectation operator. The ACF can be computed for different lags k, and the results can be plotted as autocorrelation. The plot can reveal patterns in the autocorrelation coefficients, such as a gradual decay or periodicity. Still, it cannot be used to reconstruct the original time series. After calculating the ACF, all-time series were smoothed with a moving average function with 3 data points.

2.4.1 Seasonal assessment autocorrelation function

We introduce and define the seasonal assessment autocorrelation function, $\Delta_{ACF,k}$, as a parameter to assess the AOD variation rates based on the simulated local solar radiation incidence. The equation is expressed by

$$\Delta_{\mathrm{ACF,k}} = \frac{\left(\left|\frac{\partial ACF_{\mathrm{var}}}{\partial k}\right| - \left|\frac{\partial ACF_{\mathrm{sun}}}{\partial k}\right|\right)^2}{\left(\left|\frac{\partial ACF_{\mathrm{var}}}{\partial k}\right| + \left|\frac{\partial ACF_{\mathrm{sun}}}{\partial k}\right|\right)^2}, \tag{4}$$

Where $\mathrm{ACF}_{\mathrm{var,k}}$ and $\mathrm{ACF}_{\mathrm{sun,k}}$ represent the autocorrelation time series of the variable of interest, which in this study is $\mathrm{ACF}_{\mathrm{AOD,k}}$, and of the solar radiation on k-lag days, respectively. The quantity $\Delta_{\mathrm{ACF,k}}$ is normalized and varies from 0 to 1. Values closer to zero represent a stronger similarity between the variation rate of the ACFs of the variable of interest and the solar radiation. In contrast, values closer to 1 mean decoupling between the seasonal variability of the variable of interest compared to that of solar radiation. Thus, it is possible to characterize a particular site using the average $\Delta_{\mathrm{ACF,\,k}}$, defined as $\langle\Delta_{\mathrm{ACF,\,k}}\rangle$, on the considered k-lag days. The following cases for $\langle\Delta_{\mathrm{ACF,\,k}}\rangle$ are examined:

- If $\langle\Delta_{\mathrm{ACF,\,k}}\rangle \sim 0$, the AOD and PWV seasonalities have rates of change identical to local solar radiation seasonality,
- If $\langle\Delta_{\mathrm{ACF,\,k}}\rangle \sim 1$, the AOD and PWV seasonalities are completely decoupled from the local solar radiation seasonality.

The magnitude of $\langle\Delta_{\mathrm{ACF,\,k}}\rangle$ measures the strength of the seasonal attenuation. Since this is a normalized number, it can be used to compare different sites worldwide directly. In this study, we considered a time interval of about one year, with $k = 400$ days, a statistically significant time stamp to assess the variability in the AOD and PWV autocorrelation time series.

3 Results and discussions

3.1 Temporal variability of AOD and PWV

Figure 2 shows the AOD at 500 nm and PWV time series for all selected sites. The AOD and PWV seasonal patterns are evident for all Amazonian sites. In particular, the quantitative characteristics of this behavior are already discussed in several studies (Morais et al. 2022; da Silva Palácios et al. 2020; Artaxo et al. 2022; Palácios et al. 2022). For the sites in the Amazon biome, the maximum peaks in AOD are mainly due to local and regional biomass-burning plumes, which are the main aerosol source during the dry season in the rainforest. The contrasting differences between those maximum peaks from sites in the central Amazon and those in the deforestation arc are worth noting. The sites in central Amazon (ATTO and Manaus Embrapa) are much less affected by local biomass burning, reflecting maximum AOD peaks reaching values between 1 and 1.5. In contrast, the sites in the deforestation arc (Rio Branco, Alta Floresta, Ji-Paraná, and Cuiabá) have much higher AOD values during the dry season, with peaks reaching values between 3 and 5. Interestingly, those values are even much higher than those found on the urban sites investigated in this study (La Paz, São Paulo, and Buenos Aires), showing how powerful

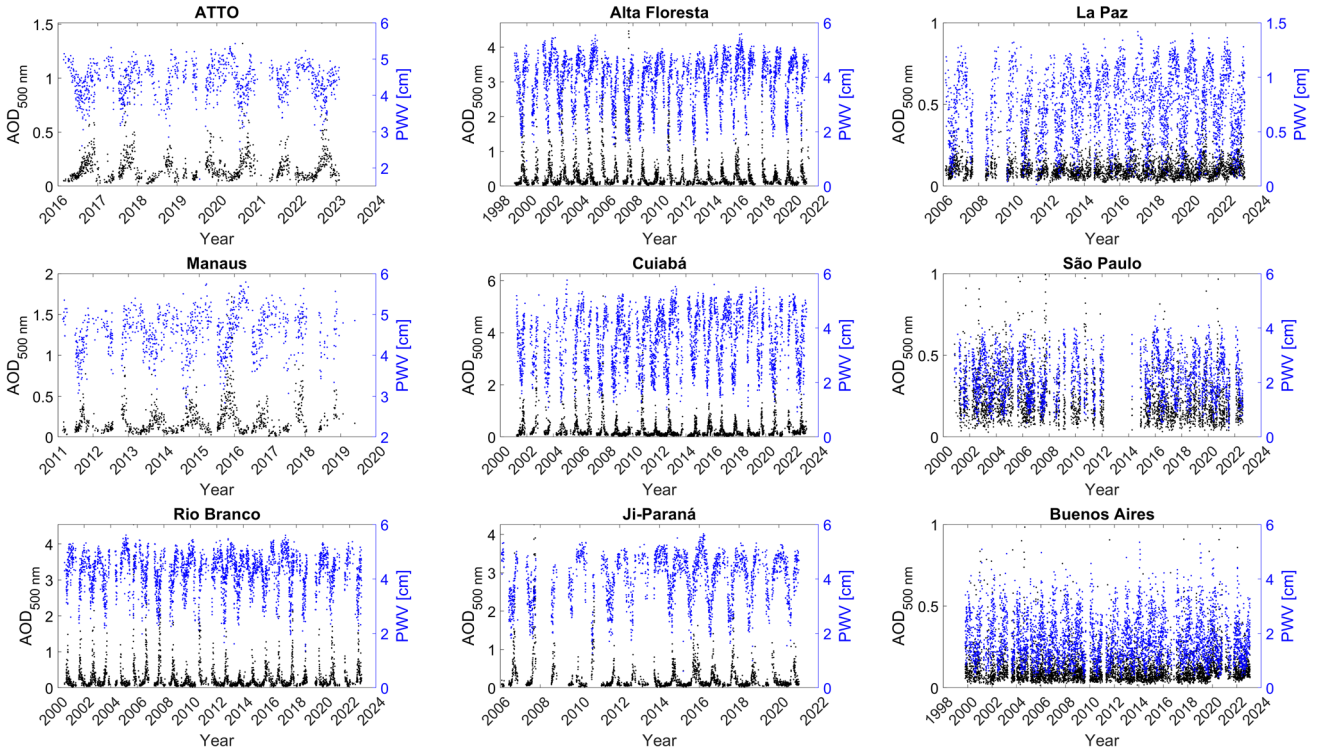

Fig. 2 AERONET AOD in 500 nm and PWV time series for all the nine sites considered in this study. Please note the different y-axis

the biomass burning events are in fueling the atmosphere with aerosols.

On the other hand, the wet deposition mechanism dominates in regulating the atmospheric aerosol population during the wet season. In the Amazon sites, the wet deposition, in addition to a strong reduction in biomass burning, drops the AOD to very low values of ~ 0.1 (Morais et al. 2022), exactly when the PWV has the higher values. For the AERONET sites in central Amazon, during this season, the atmosphere is mainly dominated by local natural sources, with primary aerosol emissions from the canopy and soil, or secondary aerosols formed directly on the atmosphere from the organic compounds also emitted by the vegetation (Andreae et al. 2018; Franco et al. 2022). Occasionally, seasonal episodic events of long-range transported aerosol plumes, e.g., from the Sahara desert, contribute to the atmospheric aerosol load. In contrast, during the wet season, the sites in the deforestation arc have two main general aerosol sources: the natural aerosols from the rainforest plus the episodic events of long-range transported aerosols, and mainly the local urban emissions. Although the intense Amazonian rain events remove those aerosols, with the increase of local sources, they can still be present in the atmosphere.

The heavily urbanized sites (La Paz, São Paulo, and Buenos Aires) show a weak AOD seasonality, much different from the other sites. There is still the presence of AOD peaks, but most of them are sporadic. In urban cities, the low aerosol seasonality may be explained by regional and long-term aerosol plume events that reach the city. For example, recently, São Paulo received a substantial biomass-burning aerosol plume from the Amazon that, together with meteorological conditions on that particular day, obfuscated the sunlight in the municipality region (Pereira et al. 2021) entirely. Also, the very low AOD seasonality may be explained by weekends and vacations, which reduces vehicular emissions. Despite that, in general, the AOD values are relatively constant throughout the year, showing that even the wet deposition cannot compete with the intense local aerosol sources, which are dominant.

3.2 AOD and PWV autocorrelations

The Eq. 2 was applied to the AOD and PWV time series considering a day lag of $k = 1000$ days, which is equivalent to about five and a half years of seasonal variability. Figure 3a shows that each site's autocorrelation series is different. Sites in the Amazon region are the ones that show more pronounced oscillations throughout the years, which is mainly driven by the biomass burning emission dynamics and the meteorological conditions of the forest, with ACF peaking at 0.3–0.5 and minimum values of ~ – 0.3. In contrast, urban sites have the lowest annual autocorrelations and oscillations. It is worth noting that the AOD ACF values for

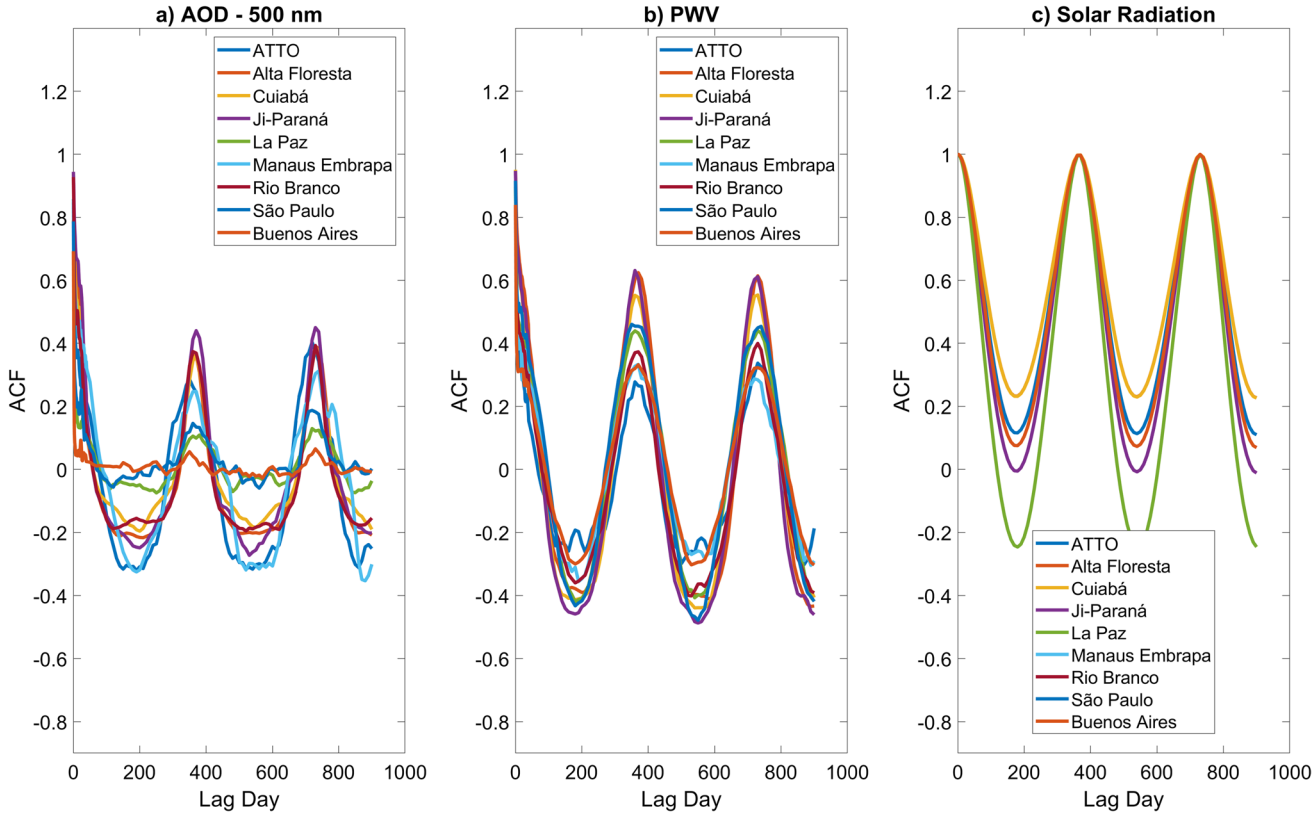

Fig. 3 Autocorrelation time series of **a** AOD500 nm, **b** PWV, and **c** direct solar radiation considering $k = 2000$

these sites oscillate around 0, with peaks of ~ 0.1 every 12 months.

Unlike the ACF AOD, the ACF PWV, presented in Fig. 3b, shows a clear seasonal pattern for all sites. The ACF PWV oscillates between negative and positive values every 6 and 12 months, respectively, with some sites with higher correlations than others, but the ACF values were not stationary around 0. The behavior of the ACF PWV has different peaks and valleys from site to site, very similar to what is observed in Fig. 3c. This depends on the meteorological conditions of each location and is not directly associated with local sources since PWV is the water vapor in the atmosphere. Figure 3c shows the seasonal pattern obtained for the simulated solar radiation. As expected, the ACF solar radiation is the unity every year after the initial start and decays for values close to or lower than zero every six months. Sites with clear ACF seasonality in AOD must also have a marked seasonality in PWV and solar radiation ACF in an ideal case. It is also important to note that the ACF does not depend directly on the absolute number of the quantity it takes into account but only on the correlation coefficient from day lags. The metric efficiently compares quantities exclusively related to the autocorrelation time series.

Figure 4 shows the ACF variability obtained for each site's AOD, PWV, and direct solar radiation time series in logarithmic x-scale. The relationship between the variables is evident. The AOD ACF in all sites follows the PWV seasonal pattern, which is directly related to the wet deposition mechanism. However, the differences in the seasonal pattern of AOD ACFs from site to site are remarkable. The AOD and PWV ACFs are very similar in central Amazonian sites, and both time series have nearly the same autocorrelations over time. It is worth noting that the mentioned behavior is also very similar to the solar radiation ACF, although the correlation magnitude is different. The ACFs smoothly decay over the first ~100 days and with the same pattern, although more minor differences are observed in Manaus Embrapa. For instance, during the first six months, the minimum ACFs were – 0.24 and – 0.30 for AOD and PWV at ATTO, respectively, and in Manaus, it was ~ – 0.32 for both ACFs, respectively. After the first 12 months, the maximum ACFs were 0.30 for both AOD and PWV at ATTO, respectively, and in Manaus, it was 0.24 and 0.33 for AOD and PWV, respectively.

The AOD, PWV, and solar radiation ACFs decay for the Amazonian deforestation arc sites also have a similar smooth pattern. However, the differences between AOD and PWV ACFs are more evident, representing clearer

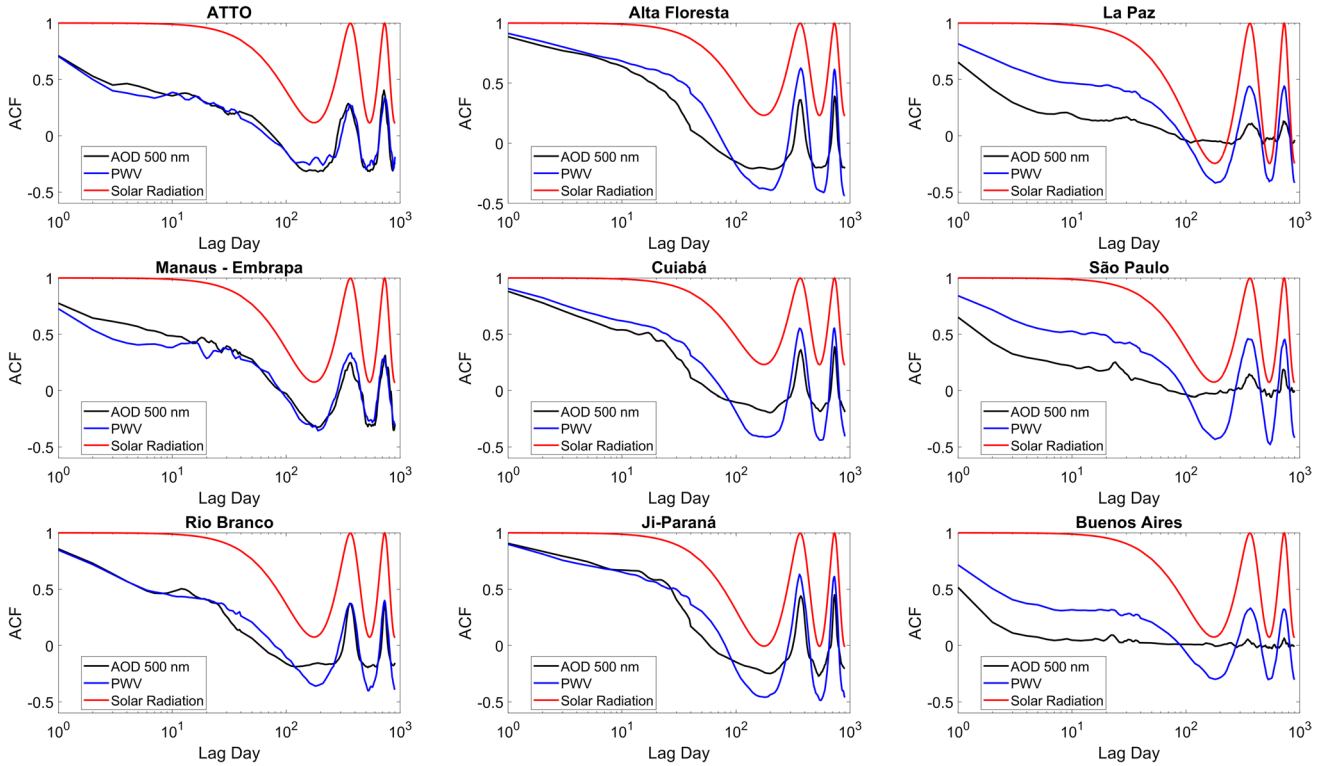

Fig. 4 ACF time series for AOD in 500 nm (black), PWV (blue), and direct solar radiation (red). The x-axis is displayed in logarithmic to improve visualization

differences between AOD and solar radiation ACFs. The AOD ACF's seasonal behavior is more attenuated than at ATTO and Manaus. The difference in the AOD and PWV autocorrelations becomes more significant, and the AOD ACF time series tends to get closer to zero when the most negative correlations are expected. After the first six months, in Rio Branco, the AOD and PWV ACFs were – 0.16 and – 0.35, respectively; in Alta Floresta, it was – 0.21 and – 0.39, respectively; in Cuiabá, it was – 0.18 and – 0.41, respectively and in Ji-Paraná it was – 0.24 and – 0.46, respectively. After 12 months, in Rio Branco, the AOD and PWV ACFs were similar, of 0.37; in Alta Floresta, it was 0.36 and 0.62, respectively; in Cuiabá, it was 0.36 and 0.55, respectively, and in Ji-Paraná it was 0.44 and 0.63, respectively. It is worth noting that the PWV autocorrelations were higher at the sites in the deforestation arc than at the central Amazon. This is likely because the precipitable water vapor in central Amazon's atmosphere is always very high, with much more complex meteorological dynamics, and varies very little compared to what is found at the deforestation arc. This means the differences between dry and wet seasons at these sites are more pronounced than in the central Amazon, which is corroborated by different studies in the literature (Smith et al. 2023).

Strongly urbanized sites show the most significant differences between AOD, PWV, and solar radiation ACFs. In particular, there is almost a complete uncoupling between the behavior of AOD and PWV ACFs in the first ~100 days. The AOD ACF tends to zero much faster than other sites. Buenos Aires has the fastest drop for oscillations, around 0. During peaks and valleys of seasonality, a minor relevance of meteorological effects is still observed in the AOD pattern but with a strongly attenuated behavior. After six months, all these sites had AOD ACF of ~ 0, while PWV ACF varied between – 0.30 and – 0.42 for Buenos Aires, São Paulo, and La Paz. After 12 months, the AOD ACF ranged between 0, 0.15, and 0.11 for Buenos Aires, São Paulo, and La Paz, and the PWV ACF ranged between 0.32, 0.46, and 0.43 for Buenos Aires, São Paulo, and La Paz, respectively. The results indicate that local aerosol processes strongly affect the seasonal AOD cycle compared to the PWV.

The relationships between AOD, PWV, and solar radiation ACFs were evaluated through linear regression between both functions and are shown in Figs. S1–S3, together with their fit statistics. Central Amazonian sites were the only ones that showed a clear linear relationship between the components in Figs. S1 and S2. As short-term perturbations become more relevant, the linearity of the relationship between AOD and PWV ACFs and AOD and solar radiation ACFs are lost.

This behavior is evident for sites in the deforestation arc, where the contribution of short-term perturbations is also significant. As the AOD ACF decreases, the autocorrelations tend to concentrate in values closer to 0, with a non-linear pattern on Figs. S1 and S2.

Linear fits were presented only to emphasize the non-linear behavior since they are inadequate for most cases. AOD ACF mitigation is even more evident in São Paulo, La Paz, and Buenos Aires. The relationships between AOD and PWV ACFs and AOD and solar radiation ACFs lose all linear behavior, and the AOD ACF component tends to concentrate on values very close to zero. At the same time, the PWV ACF continues to show oscillatory values due to its seasonality. The results show that the seasonality of AOD is increasingly attenuated as local aerosol sources become more significant. Figure S3 presents the relationship between PWV and solar radiation ACFs, where the linearity between these components is clear for all sites, with $R^2>0.95$ and p-value < 0.05. This shows that, although the linearity in the water vapor component of solar radiation, the different meteorological mechanisms that dominate in each site make the angular coefficient, a, different. Future studies may investigate in detail the possible relationships between the different meteorological mechanisms that dominate the water vapor in the atmosphere and this coefficient a, which is not within the scope of this work.

3.2.1 The influence of local aerosol processes on the AOD and PWV autocorrelation time series

The influence of short-term perturbations in modifying the seasonality pattern of the AOD and PWV time series was quantified by obtaining a point-by-point $\Delta_{ACF,\,k}$ (Eq. 4) for each site and the results are shown in Figure 5. Here, we considered $k = 400$ days, covering about one year of lag days. Since the analyzes are developed with a fixed k value, we will identify as $\langle\Delta_{ACF,\,AOD}\rangle$ and $\langle\Delta_{ACF,PWV}\rangle$ the average values obtained by Eq. 4 for AOD and PWV, respectively. Sites with constant urban emissions had the highest $\langle\Delta_{ACF,\,AOD}\rangle$, followed by sites in the deforestation arc. In contrast, the central Amazon sites were the ones that presented the lowest $\langle\Delta_{ACF,\,AOD}\rangle$, evidencing the stronger seasonal behavior of AOD compared to solar radiation. In addition, the results also allow for comparing different sites, evaluating them, and classifying them according to the degree of influence of short-term perturbations. Among the most urbanized sites, Buenos Aires was the most impacted by short-term

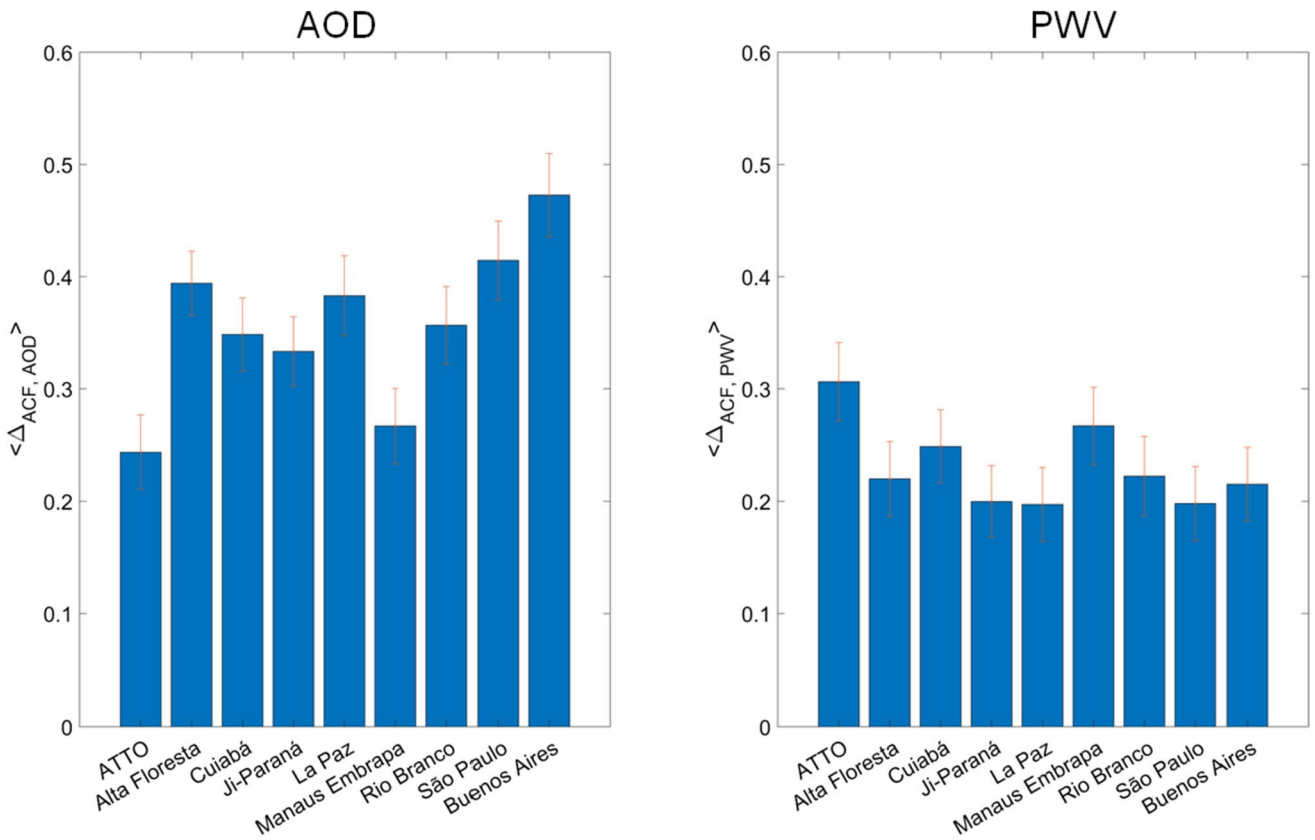

Fig. 5 Histogram of $\langle\Delta_{ACF,AOD}\rangle$ and $\langle\Delta_{ACF,PWV}\rangle$ with $k = 400$ days for each site with the mean standard deviation represented as whiskers

perturbations, followed by São Paulo and La Paz, with $\langle \Delta_{ACF,\ AOD} \rangle$ equal to 0.47, 0.42, and 0.38, respectively.

Among the sites in the deforestation arc, Alta Floresta stands out, followed by Rio Branco, Cuiabá, and Ji-Paraná, with $\langle \Delta_{ACF,AOD} \rangle$ equal to 0.39, 0.36, 0.35, and 0.33 respectively. Note that the coefficient $\langle \Delta_{ACF,AOD} \rangle$ in Alta Floresta is higher than in La Paz, which indicates that short-term perturbations at Alta Floresta, likely due to biomass burning, are more intense than the atmospheric aerosol processes in La Paz. ATTO and Manaus present $\langle \Delta_{ACF,AOD} \rangle$ equal 0.24 and 0.26, respectively. The results are consistent with what is observed in Figs. 2 and S1, demonstrating that the presented method is applicable to assess the influence of aerosol sources in regulating the AOD seasonality.

In contrast, the behavior of $\langle \Delta_{ACF,PWV} \rangle$ was different, likely due to the influence of local and regional meteorological characteristics on the seasonal pattern of precipitation. In particular, sites in the Amazon's central region had the highest values, 0.31 and 0.30, for ATTO and Manaus, respectively. However, these values are still considered low compared to AOD. The highest $\langle \Delta_{ACF,PWV} \rangle$ values in the central Amazon region are associated with a large amount of water vapor present throughout the year, although its seasonality is well known (Franco et al. 2022). However, the situation varies according to the location of the study points, especially in the vicinity of the deforestation arc and large cities, where $\langle \Delta_{ACF,PWV} \rangle$ values are very close. Seasonality is more evident in these areas, with oscillation amplitudes seen in Fig. 4 higher than those in the Amazon's central region.

4 Conclusions

This study proposes a new approach to evaluate the AOD and PWV seasonality and the influence of local aerosol processes on AOD seasonal behavior. The seasonal assessment autocorrelation function, $\Delta_{ACF,k}$, was introduced and defined as a parameter to quantify the influence of short-term influences on AOD and PWV seasonality regardless of reference sites. Nine sites from the AERONET network located in South America with differing environmental characteristics, such as forested, urban, and heavily urbanized areas, were selected for the study and proof of concept. It was observed that sites with a cleaner atmosphere and less anthropogenic emissions displayed more significant AOD seasonality and a linear relationship between AOD and PWV autocorrelation functions. In contrast, as local anthropogenic sources increase, the AOD autocorrelation function smooths and exhibits less amplitude in seasonal oscillations and a loss of linearity compared to the PWV autocorrelation function. The heavily urbanized sites demonstrated this behavior, with AOD autocorrelation values close to zero regardless of the number of lag days considered. Buenos Aires was the most impacted site, followed by São Paulo and La Paz. The sites in the deforestation arc had relatively similar $\langle \Delta_{ACF,AOD} \rangle$, with Alta Floresta having the highest, which is even higher than the one for La Paz. Of the sites in central Amazon, both $\langle \Delta_{ACF,\ AOD} \rangle$ were very similar, of ~0.25, with Manaus showing a slightly higher value likely due to urban emissions reaching the site. In contrast, $\langle \Delta_{ACF,\ PWV} \rangle$ displays a different behavior compared to $\langle \Delta_{ACF,\ AOD} \rangle$, likely due to local and regional meteorological influences on precipitation seasonality. The central region of the Amazon shows the highest values, with ATTO and Manaus recording 0.31 and 0.30, respectively, although these values are still relatively low compared to AOD peaks. In areas near deforestation arcs and bigger cities, $\langle \Delta_{ACF,\ PWV} \rangle$ values are similar and demonstrate more pronounced seasonality. The study's results were robust and consistent with the seasonal behavior of the AOD and the expected results based on the chosen study sites. This new method provides a quantitative approach to assessing the influence of local aerosol processes on AOD seasonality, allowing for comparison between different sites. Moreover, the technique has the potential to be applied to other atmospheric time series, such as the seasonality of greenhouse gases, black carbon aerosols, and many different meteorological variables.

Supplementary Information The online version contains supplementary material available at https://doi.org/10.1007/s00703-024-01011-5.

Acknowledgements MAF and MT acknowledge the Fundação de Amparo à Pesquisa do Estado de São Paulo FAPESP, projects 2021/13610-8 and 2021/12954-5, respectively, for financial support. MAF acknowledges the Conselho Nacional de Desenvolvimento Científico e Tecnológico (CNPq) Universal project number 407752/2023-4 for financial support. Authors acknowledge the support of the Research Centre for Greenhouse Gas Innovation (RCGI), hosted by the University of São Paulo (USP) and sponsored by the São Paulo State Research Foundation (FAPESP) (grants 2014/50279-4 and 2020/15230-5) and Shell Brasil, and the strategic importance of the support given by Brazil's National Oil, Natural Gas and Biofuels Agency (ANP) through the R &D levy regulation.

Author contributions MAF designed the study and wrote the paper. FGM, LVR, RP, RV, MT, LATM, and PA contributed to the data analysis. All authors contributed to the discussion of the results as well as the finalization of the manuscript.

Funding This article is funded by Fundação de Amparo à Pesquisa do Estado de São Paulo (2021/13610- 8, 2021/12954-5, 2014/50279-4 and 2020/15230-5) and Conselho Nacional de Desenvolvimento Científico e Tecnológico (07752/2023-4).

Data availability Data available under correspondent author's request.

Code availability All codes are available under the author's request.

Declarations

Conflict of interest The authors declare that they have no known Conflict of interest that could have influenced the work reported in this paper.

References

Abe KC, Miraglia SGEK (2016) Health impact assessment of air pollution in São Paulo, Brazil. Int J Environ Res Public Health 13:694

Alvares CA, Stape JL, Sentelhas PC, Gonçalves JDM, Sparovek G (2013) Köppen's climate classification map for Brazil. Meteorologische Zeitschrift 22:711–728

Andreae MO, Acevedo OC, Araùjo A, Artaxo P, Barbosa CGG, Barbosa HMJ, Brito J, Carbone S, Chi X, Cintra BBL, da Silva NF, Dias NL, Dias-Júnior CQ, Ditas F, Ditz R, Godoi AFL, Godoi RHM, Heimann M, Hoffmann T, Kesselmeier J, Könemann T, Krüger ML, Lavric JV, Manzi AO, Lopes AP, Martins DL, Mikhailov EF, Moran-Zuloaga D, Nelson BW, Nölscher AC, Santos Nogueira D, Piedade MTF, Pöhlker C, Pöschl U, Quesada CA, Rizzo LV, Ro C-U, Ruckteschler N, Sá LDA, de Oliveira Sá M, Sales CB, dos Santos RMN, Saturno J, Schöngart J, Sörgel M, de Souza CM, de Souza RAF, Su H, Targhetta N, Tóta J, Trebs I, Trumbore S, van Eijck A, Walter D, Wang Z, Weber B, Williams J, Winderlich J, Wittmann F, Wolff S, Yáñez Serrano AM (2015) The Amazon Tall Tower Observatory (ATTO): overview of pilot measurements on ecosystem ecology, meteorology, trace gases, and aerosols. Atmos Chem Phys 15:10723–10776. https://doi.org/10.5194/acp-15-10723-2015

Andreae MO, Afchine A, Albrecht R, Holanda BA, Artaxo P, Barbosa HMJ, Borrmann S, Cecchini MA, Costa A, Dollner M, Fütterer D, Järvinen E, Jurkat T, Klimach T, Konemann T, Knote C, Krämer M, Krisna T, Machado LAT, Mertes S, Minikin A, Pöhlker C, Pöhlker ML, Pöschl U, Rosenfeld D, Sauer D, Schlager H, Schnaiter M, Schneider J, Schulz C, Spanu A, Sperling VB, Voigt C, Walser A, Wang J, Weinzierl B, Wendisch M, Ziereis H (2018) Aerosol characteristics and particle production in the upper troposphere over the Amazon Basin. Atmos Chem Phys 18:921–961. https://doi.org/10.5194/acp-18-921-2018

Artaxo P, Martins JV, Yamasoe MA, Procópio AS, Pauliquevis TM, Andreae MO, Guyon P, Gatti LV, Leal AMC (2002) Physical and chemical properties of aerosols in the wet and dry seasons in Rondônia, Amazonia. J Geophys Res: Atmos 107:LBA-49

Artaxo P, Hansson H-C, Andreae MO, Bäck J, Alves EG, Barbosa HM, Bender F, Bourtsoukidis E, Carbone S, Chi J et al (2022) Tropical and boreal forest atmosphere interactions: a review, Tellus. Chemical and Physical Meteorology, Series B Chemical and Physical Meteorology 74(1):24–163. https://doi.org/10.16993/tellusb.34

Bernstein JA, Alexis N, Barnes C, Bernstein IL, Nel A, Peden D, Diaz-Sanchez D, Tarlo SM, Williams PB (2004) Health effects of air pollution. J Allergy Clin Immunol 114:1116–1123

Borsdorf A, Haller A (2020) Urban montology: mountain cities as transdisciplinary research focus. The Elgar companion to geography, transdisciplinarity and sustainability. Edward Elgar Publishing, Cheltenham, pp 140–154

Brito J, Carbone S, Monteiro A, dos Santos D, Dominutti P, de Oliveira Alves N, Rizzo VL, Artaxo P (2018) Disentangling vehicular emission impact on urban air pollution using ethanol as a tracer. Sci. Rep 8:1–10

Carra E, Marzo A, Ballestrín J, Polo J, Barbero J, Alonso-Montesinos J, Monterreal R, Abreu EF, Fernández-Reche J (2020) Atmospheric extinction levels of solar radiation using aerosol optical thickness satellite data. Validation Methodol Meas Syst Renew Energy 149:1120–1132

Carracedo-Martínez E, Taracido M, Tobias A, Saez M, Figueiras A (2010) Case-crossover analysis of air pollution health effects: a systematic review of methodology and application. Environ Health Perspect 118:1173–1182

Chau K, Franklin M, Lee H, Garay M, Kalashnikova O (2021) Temporal and spatial autocorrelation as determinants of regional AOD-PM2. 5 model performance in the Middle East. Remote Sens 13:3790

Cheung H-C, Wang T, Baumann K, Guo H (2005) Influence of regional pollution outflow on the concentrations of fine particulate matter and visibility in the coastal area of southern China. Atmos Environ 39:6463–6474

Chu Y, Liu Y, Li X, Liu Z, Lu H, Lu Y, Mao Z, Chen X, Li N, Ren M et al (2016) A review on predicting ground PM2. 5 concentration using satellite aerosol optical depth. Atmosphere 7:129

Cuneo L, Ulke AG, Cerne B (2022) Advances in the characterization of aerosol optical properties using long-term data from AERONET in Buenos Aires. Atmos Pollut Res 13:101–360

da Silva Palácios R, Romera KS, Curado LFA, Banga NM, Rothmund LD, da Silva Sallo F, Morais D, Santos ACA, Moraes TJ, Morais FG et al (2020) Long term analysis of optical and radiative properties of aerosols in the Amazon Basin. Aerosol Air Qual Res 20:139–154

de Fatima Andrade M, Kumar P, de Freitas ED, Ynoue RY, Martins J, Martins LD, Nogueira T, Perez-Martinez P, de Miranda RM, Albuquerque T et al (2017) Air quality in the megacity of São Paulo: evolution over the last 30 years and future perspectives. Atmos Environ 159:66–82

dos Santos DAM, Brito JF, Godoy JM, Artaxo P (2016) Ambient concentrations and insights on organic and elemental carbon dynamics in São Paulo, Brazil. Atmos Environ 144:226–233

Dubovik O, Sinyuk A, Lapyonok T, Holben BN, Mishchenko M, Yang P, Eck TF, Volten H, Munoz O, Veihelmann B et al (2006) Application of spheroid models to account for aerosol particle nonsphericity in remote sensing of desert dust. Journal of Geophysical Research: Atmospheres, 111:D11208

Franco MA, Ditas F, Kremper LA, Machado LA, Andreae MO, Araújo A, Barbosa HM, de Brito JF, Carbone S, Holanda BA et al (2022) Occurrence and growth of sub-50 nm aerosol particles in the Amazonian boundary layer. Atmos Chem Phys 22:3469–3492

Hair JF (2011) Multivariate data analysis: An overview, International encyclopedia of statistical science, pp 904–907. https://link.springer.com/referenceworkentry/10.1007%2F978-3-642-04898-2_395

Holanda BA, Pöhlker ML, Walter D, Saturno J, Sörgel M, Ditas J, Ditas F, Schulz C, Franco MA, Wang Q et al (2020) Influx of African biomass burning aerosol during the Amazonian dry season through layered transatlantic transport of black carbon-rich smoke. Atmos Chems Phys 20:4757–4785

Holanda BA, Franco MA, Walter D, Artaxo P, Carbone S, Cheng Y, Chowdhury S, Ditas F, Gysel-Beer M, Klimach T et al (2023) African biomass burning affects aerosol cycling over the Amazon. Commun Earth Environ 4:154

Holben BN, Eck TF, Slutsker IA, Tanre D, Buis J, Setzer A, Vermote E, Reagan JA, Kaufman Y, Nakajima T (1998) AERONET-A federated instrument network and data archive for aerosol characterization. Remote Sens Environ 66:1–16

Hua W, Junfeng Z, Fubao Z, Weiwei Z (2016) Analysis of spatial pattern of aerosol optical depth and affecting factors using spatial autocorrelation and spatial autoregressive model. Environ Earth Sci 75:1–17

INDEC A (2010) Censo nacional de población, hogares y vivienda, República Argentina: Inst Nac Estadísticay Censos. https://bit.ly/2LHKHff

Jin X, Fiore AM, Curci G, Lyapustin A, Civerolo K, Ku M, Van Donkelaar A, Martin RV (2019) Assessing uncertainties of a geophysical approach to estimate surface fine particulate matter distributions from satellite-observed aerosol optical depth. Atmos Chem Phys 19:295–313

Kambezidis H, Kaskaoutis D (2008) Aerosol climatology over four AERONET sites: an overview. Atmos Environ 42:1892–1906

Kampa M, Castanas E (2008) Human health effects of air pollution. Environ Pollut 151:362–367

Kaskaoutis D, Kambezidis H, Hatzianastassiou N, Kosmopoulos P, Badarinath K (2007) Aerosol climatology: on the discrimination of aerosol types over four AERONET sites. Atmos Chemis Phys Discuss 7:6357–6411

Manisalidis I, Stavropoulou E, Stavropoulos A, Bezirtzoglou E (2020) Environmental and health impacts of air pollution: a review. Frontiers in public health 8:14. https://doi.org/10.3389/fpubh.2020.00014

Mardoñez V, Pandolfi M, Borlaza LJS, Jaffrezo JL, Alastuey A, Besombes JL, Moreno RI, Perez N, Močnik G, Ginot P, et al (2022) Source apportionment study on particulate air pollution in two high-altitude Bolivian cities: La Paz and El Alto. Atmospheric Chemistry and Physics Discussions 23(18):10325–10347

Monteiro dos Santos D, Rizzo LV, Carbone S, Schlag P, Artaxo P (2021) Physical and chemical properties of urban aerosols in São Paulo, Brazil: links between composition and size distribution of submicron particles. Atmos Chem Phys 21:8761–8773

Morais FG, Franco MA, Palácios R, Machado LA, Rizzo LV, Barbosa HM, Jorge F, Schafer JS, Holben BN, Landulfo E et al (2022) Relationship between land use and spatial variability of atmospheric brown carbon and black carbon aerosols in Amazonia. Atmosphere 13:1328

Næss Ø, Nafstad P, Aamodt G, Claussen B, Rosland P (2007) Relation between concentration of air pollution and cause-specific mortality: four-year exposures to nitrogen dioxide and particulate matter pollutants in 470 neighborhoods in Oslo, Norway. Am J Epidemiol 165:435–443

Nascimento JP, Bela MM, Meller BB, Banducci AL, Rizzo LV, Vara-Vela AL, Barbosa HM, Gomes H, Rafee SA, Franco MA et al (2021) Aerosols from anthropogenic and biogenic sources and their interactions-modeling aerosol formation, optical properties, and impacts over the central Amazon basin. Atmos Chem Phys 21:6755–6779

Nascimento JP, Barbosa HM, Banducci AL, Rizzo LV, Vara-Vela AL, Meller BB, Gomes H, Cezar A, Franco MA, Ponczek M et al (2022) Major regional-scale production of O3 and secondary organic aerosol in remote amazon regions from the dynamics and photochemistry of urban and forest emissions. Environ Sci Technol 56:9924–9935

Nworof O, Chineka T (2007) Mathematical representation of seasonal cycles of aerosol optical depths at Ilorin Nigeria using AERONET data. Global J Pure Appl Sci 13:285–294

Oliveira M, Drumond A, Rizzo L (2022) Air pollution persistent exceedance events in the Brazilian metropolis of Sao Paulo and associated surface weather patterns. Int J Environ Sci Technol 19:9495–9506

Palácios R, Nassarden DC, Franco MA, Morais FG, Machado LA, Rizzo LV, Cirino G, Pereira AG, Ribeiro PDS, Barros LR (2022) Evaluation of MODIS Dark Target AOD Product with 3 and 10 km Resolution in Amazonia. Atmosphere 13:1742

Pereira GM, da Silva Caumo SE, Grandis A, Do Nascimento EQM, Correia AL, Barbosa HDMJ, Marcondes MA, Buckeridge MS, de Castro Vasconcellos P (2021) Physical and chemical characterization of the (2019) Physical and chemical characterization of the 2019 Black rain event in the Metropolitan Area of Sao Paulo, Brazil. Atmos Environ 248:118–229

Ponczek M, Franco MA, Carbone S, Rizzo LV, dos Santos DM, Morais FG, Duarte A, Barbosa HM, Artaxo P (2022) Linking the chemical composition and optical properties of biomass burning aerosols in Amazonia. Environ Sci: Atmos 2:252–269

Prasad AK, Singh RP (2009) Validation of MODIS Terra, AIRS, NCEP/DOE AMIP-II Reanalysis-2, and AERONET Sun photometer derived integrated precipitable water vapor using ground-based GPS receivers over India. Journal of Geophysical Research: Atmospheres 114:D05107. https://doi.org/10.1029/2008JD011230

Reda I, Andreas A (2004) Solar position algorithm for solar radiation applications. Solar Energy 76:577–589

Ribeiro AG, Downward GS, de Freitas CU, Neto FC, Cardoso MRA, Hystad MDRD, Hystad P, Vermeulen R, Nardocci AC (2019) Incidence and mortality for respiratory cancer and traffic-related air pollution in São Paulo, Brazil. Environ Res 170:243–251

Seinfeld JH, Pandis SN (2016) Atmospheric chemistry and physics: from air pollution to climate change. John Wiley and Sons, Hoboken

Smith C, Baker J, Spracklen D (2023) Tropical deforestation causes large reductions in observed precipitation. Nature 615(7951):270–275

Stafford B (2015) Stafford Brandon Pysolar documentation. https://doi.org/10.5281/zenodo.1461066, https://pysolar.readthedocs.io/

Tiwari S, Payra S, Mohan M, Verma S, Bisht DS (2011) Visibility degradation during foggy period due to anthropogenic urban aerosol at Delhi, India. Atmos Pollut Res 2:116–120

Wiedensohler A, Andrade M, Weinhold K, Müller T, Birmili W, Velarde F, Moreno I, Forno R, Sanchez M, Laj P et al (2018) Black carbon emission and transport mechanisms to the free troposphere at the La Paz/El Alto (Bolivia) metropolitan area based on the Day of Census (2012). Atmos Environ 194:158–169

Yang J, Hu M (2018) Filling the missing data gaps of daily MODIS AOD using spatiotemporal interpolation. Sci Total Environ 633:677–683

Zhao TX, Stowe LL, Smirnov A, Crosby D, Sapper J, McClain CR (2002) Development of a global validation package for satellite oceanic aerosol optical thickness retrieval based on AERONET observations and its application to NOAA/NESDIS operational aerosol retrievals. J Atmos Sci 59:294–312